J|A|C|S
ARTICLES
Published on Web 02/02/2008

# Selective Oxidation on Metallic Carbon Nanotubes by Halogen Oxoanions

Seon-Mi Yoon,[†] Sung Jin Kim,[‡] Hyeon-Jin Shin,[†] Anass Benayad,[†] Seong Jae Choi,[†] Ki Kang Kim,[‡] Soo Min Kim,[‡] Yong Jin Park,[‡] Gunn Kim,[‡] Jae-Young Choi,*[,†] and Young Hee Lee*[,‡]

*Display Device & Processing Lab and Analytical Engineering Center, Samsung Advanced Institute of Technology, Post Office Box 111, Suwon 440-600, Korea, and Department of Physics, Department of Nanoscience and Nanotechnology, and Center for Nanotubes and Nanostructured Composites, Sungkyunkwan Advanced Institute of Nanotechnology, Sungkyunkwan University, Suwon 440-746, Korea*

Received September 27, 2007; E-mail: jaeyoung88.choi@saumsung.com (J.-Y.C.); leeyoung@skku.edu (Y.H.L.)

***Abstract:*** Chlorine oxoanions with the chlorine atom at different oxidation states were introduced in an attempt to systematically tailor the electronic structures of single-walled carbon nanotubes (SWCNTs). The degree of selective oxidation was controlled systematically by the different oxidation state of the chlorine oxoanion. Selective suppression of the metallic SWCNTs with a minimal effect on the semiconducting SWCNTs was observed at a high oxidation state. The adsorption behavior and charge transfer at a low oxidation state were in contrast to that observed at a high oxidation state. Density functional calculations demonstrated the chemisorption of chloro oxoanions at the low oxidation state and their physisorption at high oxidation states. These results concurred with the experimental observations from X-ray photoelectron spectroscopy. The sheet resistance of the SWCNT film decreased significantly at high oxidation states, which was explained in terms of a p-doping phenomenon that is controlled by the oxidation state.

## 1. Introduction

Modification of the atomic and electronic structures of carbon nanotubes is a crucial step in many applications.[1] Strong chemical bonding between the host materials and carbon nanotubes is essential for enhancing the mechanical properties of the host materials, whereas a simple dispersion of nanotubes in a host matrix can enhance the conductivity of the host materials.[2] Functionalization of single-walled carbon nanotubes (SWCNTs) by hydrogenation and fluorination leads to a significant change not only in the atomic structures but also in the electronic structures of carbon nanotubes.[3,4] Doping control of carbon nanotubes by various chemical means is also strongly dependent on the types of chemical dopants.[5] Various dispersants have been used to disperse carbon nanotubes. This often involves serious modification of the electronic structures of the carbon nanotubes.[1] The presence of functional groups in the dispersant may induce a permanent or an induced dipole moment in a molecular solvent. This presumably involves charge transfer between the absorbates and carbon nanotubes, which modifies the electronic structures of the carbon nanotubes. In order to tailor the electronic structures of carbon nanotubes to a desired direction, it is essential to understand the effect of the absorbates.

Halogen oxoanions are a systematic oxidant in engineering redox reactions due to the existence of different oxidation states. As the oxidation state of the halogen oxoanions increases, the number of electrons participating in its redox reaction increases, whereas the redox potential of the reaction decreases.[6] Most oxidants can be used as a p-dopant in carbon nanotubes. For example, $SOCl_2$, iodine, and a simple acid treatment enhance the majority carrier concentration and increase the conductivity of carbon nanotubes (CNTs).[7−10] This trend can be altered depending on the physisorption or chemisorption states of the adsorbates. Nevertheless, an understanding of the oxidation of CNTs and their related physical and chemical properties are still unclear. Chlorine oxoacids can provide useful information on the doping of CNTs in this matter, which can be engineered by different oxidation states with the same chlorine atoms. In general, a wide range of oxidation states is more easily found in oxidants with chlorine atoms than those with other halogen atoms.[6] Therefore, the effect of oxidation by chlorine oxoanions can be correlated exclusively with the electronic structures of the CNTs.

[†] SAIT.
[‡] Sungkyunkwan University.

(1) Tasis, D.; Tagmatarchis, N.; Bianco, A.; Prato, M. *Chem. Rev.* **2006**, *106*, 1105.
(2) Hu, Y.; Shenderova, O.; Hu, Z.; Padgett, C. W.; Brenner, D. W. *Rep. Prog. Phys.* **2006**, 1847.
(3) Nikitin, A.; Ogasawara, H.; Mann, D.; Denecke, R.; Zhang, Z.; Dai, H.; Cho, K.; Nilsson, A. *Phys. Rev. Lett.* **2005**, *95*, 225507.
(4) Peng, H.; Reverdy, P.; Khabashesku, V. N.; Margrave, J. L. *Chem. Commun.* **2003**, 362.
(5) (a) Chen, J.; Hamon, M. A.; Hu, H.; Chen, Y.; Rao, A. M.; Eklund, P. C.; Haddon, R. C. *Science* **1998**, *282*, 95. (b) Zhou, C.; Kong, J.; Yenilmez, E.; Dai, H. *Science* **2000**, *290*, 1552.
(6) (a) Shriver, D. F.; Atkins, P. W. *Inorganic Chemistry*; Oxford University Press: Oxford, U.K., 1999; Chapt. 12, pp 405−429. (b) *Handbook of Chemistry and Physics*; CRC Press: Boca Raton, FL, 2005.
(7) Dettlaff-Weglikowska, U.; Skákalová, V.; Graupner, R.; Jhang, S. H.; Kim, B. H.; Lee, H. J.; Ley, L.; Park, Y. W.; Berber, S.; Tománek, D.; Roth, S. *J. Am. Chem. Soc.* **2005**, *127*, 5125.
(8) Rao, A. M.; Eklund, P. C.; Bandow, S.; Thess, T.; Smalley, R. E. *Nature* **1997**, *388*, 257.
(9) Itkis, M. E.; Niyogi, S.; Meng, M. E.; Hamon, M. A.; Hu, H.; Haddon, R. C. *Nano Lett.* **2002**, *2*, 155.
(10) Geng, H.-Z.; Kim, K. K.; So, K. P.; Lee, Y. S.; Chang, Y.; Lee, Y. H. *J. Am. Chem. Soc.* **2007**, *129*, 7758.


**10.1021/ja077449d CCC: $40.75** 

***Table 1.*** Material Parameters of the Chlorine Oxoanions[6] [a]

| Oxidation number | Formula | Name | Reaction | $E^0$, V | Structure |
|---|---|---|---|---|---|
| +1 | $ClO^-$ | Hypochlorite [monoxochlorate (I)] | $ClO^- + H_2O + 2\,e \leftrightarrow Cl^- + 2\,OH^-$ | 0.81 |  |
| +3 | $ClO_2^-$ | Chlorite [dioxochlorate (III)] | $ClO_2^- + H_2O + 2\,e \leftrightarrow ClO^- + 2\,OH^-$<br>$ClO_2^- + 2\,H_2O + 4\,e \leftrightarrow Cl^- + 4\,OH^-$ | 0.66<br>0.76 |  |
| +5 | $ClO_3^-$ | Chlorate [trioxochlorate (V)] | $ClO_3^- + H_2O + 2\,e \leftrightarrow ClO_2^- + 2\,OH^-$<br>$ClO_3^- + 3\,H_2O + 6\,e \leftrightarrow Cl^- + 6\,OH^-$ | 0.33<br>0.62 |  |
| +7 | $ClO_4^-$ | Perchlorate [tetraoxochlorate (VII)] | $ClO_4^- + H_2O + 2\,e \leftrightarrow ClO_3^- + 2\,OH^-$ | 0.36 |  |

[a] $E^0$ indicates the standard redox potential.

The aim of this study was to determine how the electronic structures of CNTs can be engineered systematically by oxidants. In this paper, chlorine oxoanions with different oxidation states were introduced to correlate the degree of oxidation with the electronic structures of the CNTs. Raman spectroscopy showed that metallic SWCNTs were selectively doped at a high oxidation state without any significant modification of the semiconducting SWCNTs. In addition, the degree of doping was controlled by the oxidation state. X-ray photoelectron spectroscopy (XPS) and density functional calculations demonstrated that physisorption was involved at a high oxidation state and selective doping on the metallic nanotubes was observed, whereas chemisorption played an important role in modifying the electronic structures of the CNTs at a low oxidation state.

## 2. Sample Preparation and Experimental and Theoretical Methods

SWCNTs were synthesized by arc discharge and purchased from Iljin Nanotech Co. Ltd. The chloro oxoanion sodium salts ($NaClO_x$) were dissolved in deionized water to produce a 20% aqueous solution. This aqueous $NaClO_x$ solution of 0.0161 M was further dissolved in 10 mL of 1-methyl-2-pyrrolidinone (NMP) solution. One milligram of the SWCNTs was then added to the mixed solution, which was sonicated in a bath-type sonicator (Bandelin Sonorex) at 240 W for 10 h. This solution was filtered through an anodisc filter (Whatman Ltd.) with a pore size of 0.1 $\mu$m. The CNTs film was dried at room temperature overnight. The sheet resistance at room temperature was measured by use of a four-point probe (AIT Co. Ltd., SR1000N). The CNT films were characterized by micro-Raman spectroscopy (Renishaw RM1000-Invia). Two excitation energies of 2.41 eV (514 nm, $Ar^+$ ion laser), 1.96 eV (632.8 nm, He−Ne laser) with a Rayleigh line rejection filter, which accepts a spectral range of 50∼3200 $cm^{-1}$ were used in this study. XPS analysis (Quantum 2000, Physical electronics) with focused monochromatized Al K$\alpha$ radiation (1486.6 eV) was carried out to check for the presence of residual material and the degree of doping effect.

Ab initio electronic structure calculations were performed to further understand the experimental findings. The ClO molecule with a low oxidation state and the $ClO_4$ molecule with a high oxidation were absorbed on (5,5) nanotubes to examine the adsorption behavior. The density functional theory (DFT) within the local density approximation (LDA) for the exchange−correlation energy was adopted. Norm-conserving Kleinman−Bylander pseudopotentials[11,12] were employed, and the wave functions were expanded by use of a numerical atomic orbital basis set in OpenMX code[13,14] with a kinetic energy cutoff of 120 Ry. In this basis set, the 2s and 2p orbitals of carbon, oxygen, and chlorine are represented by two functions, respectively. The supercell in the lateral direction was as large as 20 Å and contained 6 times the minimal unit cell (∼2.46 Å) along the tube axis. The geometries were optimized until the Hellmann−Feynman forces were <0.02 eV/Å. Some calculations were repeated with the DMol3 package,[15] which led to similar results.

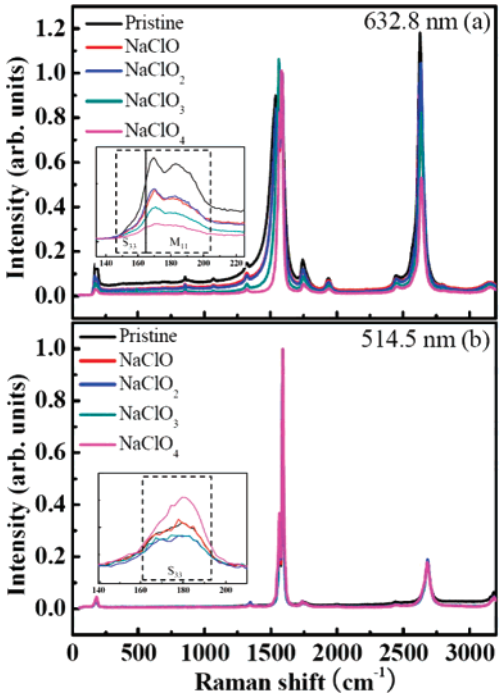


***Figure 1.*** Raman spectra at an excitation of (a) 633 and (b) 514 nm of the pristine and chloro oxoanion-treated samples at different oxidation states before heat treatment. The intensities of the radial breathing modes decreased with increasing oxidation state at an excitation energy of 1.96 eV, whereas they were rather enhanced at 2.41 eV. Each spectrum was averaged over several points of the sample. No significant deviation was observed from point to point.

## 3. Results and Discussion

Chlorine oxoanions are commonly available halogen species with various oxidation states. Table 1 shows the material parameters of the chlorine oxoanions with the various oxidation states used in this study. At a low oxidation state, the redox potential is high, and thus the reaction is thermodynamically favored. The number of electrons participating in the reaction increases with increasing oxidation states, as shown in Table 1. This number of electrons involved in the redox reaction, together with redox potential, can be correlated exclusively with the doped state of the CNTs.

Figure 1 shows the Raman spectra of various samples treated with chlorine oxoanions. At an excitation energy of 633 nm (1.96 eV), the metallic SWCNTs were mainly excited in the pristine sample (thick solid line), as shown in the radial breathing modes (RBMs) in the inset. The abundance of the metallic component was confirmed by the large portion of the Breit−Wigner−Fano (BWF) line of the G-band that represents a long energy tail at a lower energy side in the pristine sample.[16] This metallic component decreased gradually with increasing oxidation state, and the BWF line profile disappeared at oxidation states of +5 and +7. The two main peaks in RBMs represented the abundance of the metallic nanotubes. These peaks were gradually reduced with increasing oxidation states, in consistent with the reduction of BWF line. On the other hand, at an excitation energy of 514 nm (2.41 eV), the semiconducting

(11) Troullier, N.; J. L.; Martins, J. L. *Phys. Rev. B* **1991**, *43*, 1993.
(12) Kleinman, L.; Bylander, D. M. *Phys. Rev. Lett.* **1982**, *48*, 1425.
(13) Ozaki, T. *Phys. Rev. B* **2003**, *67*, 55108.
(14) Ozaki, T.; Kino, H. *Phys. Rev. B* **2004**, *69*, 195113.
(15) The Dmol3 is a registered software product of Accelrys, Inc.
(16) Jorio, A.; Souza Filho, A. G.; Dresselhaus, G.; Dresselhaus, M. S.; Swan, A. K.; Unlu, M. S.; Goldberg, B. B.; Pimenta, M. A.; Hafner, J. H.; Lieber, C. M.; Saito, R. *Phys. Rev. B* **2002**, *65*, 155412.

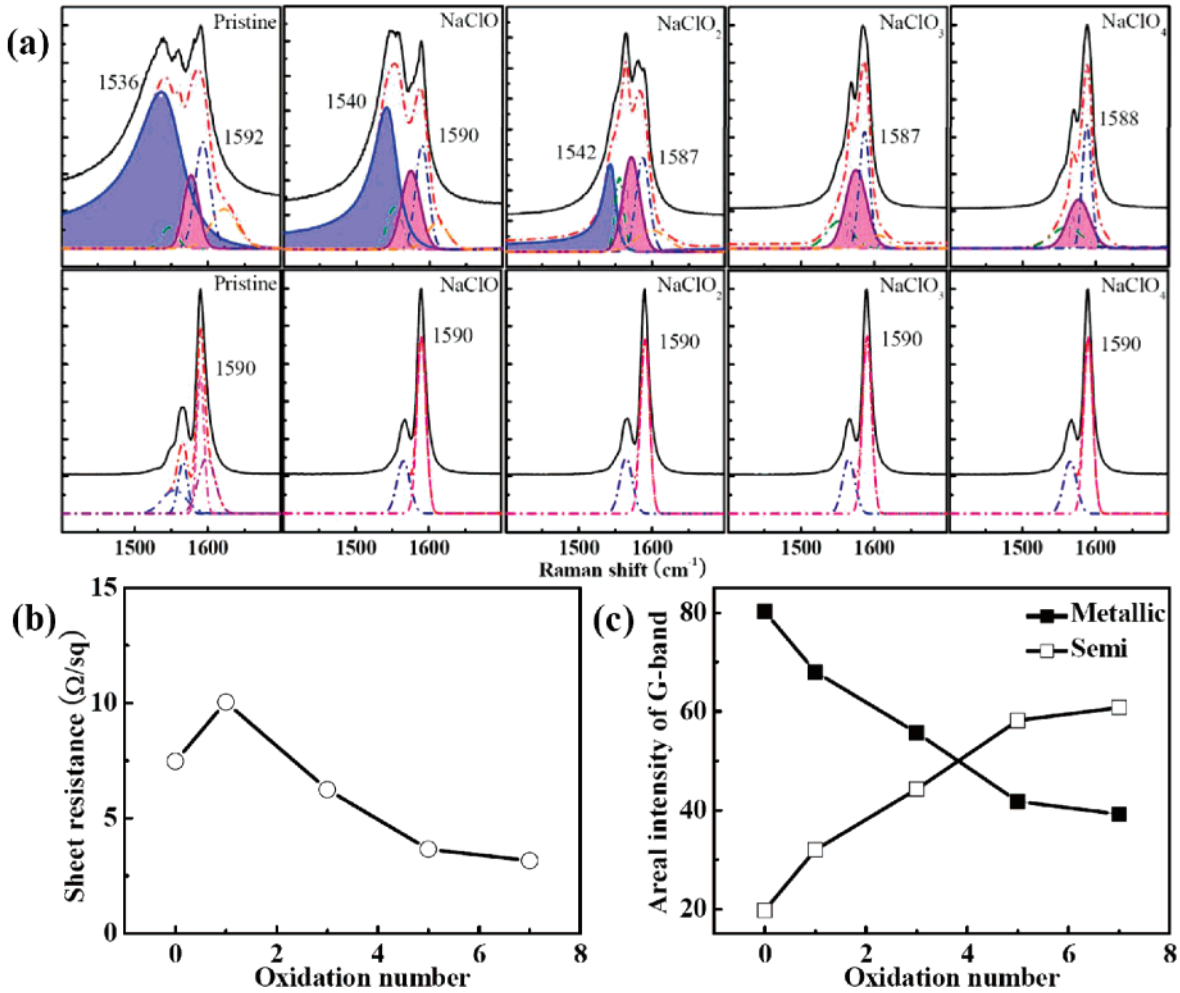


***Figure 2.*** (a) Raman spectra at 633 and 514 nm of the chloro oxoanion-treated samples at different oxidation states. The G-band was deconvoluted into two metallic and four semiconducting components. The shaded regions at 633 nm excitation indicate the BWF line (left) and the metallic component (right). The numbers in the figure indicate the peak positions of the $G^+$-band (also BWF peak positions). (b) Sheet resistance and (c) relative areal intensity of the metallic and semiconducting components with respect to the whole areal intensity of the G-band at 1.96 eV in terms of the oxidation state.

SWCNTs were excited exclusively; that is, neither the BWF line shape in G-band nor the metallic component in the RBMs was observed. In this case, there were no appreciable changes in G-band and RBMs, which is in contrast with those observed at 633 nm. Understanding the underlying mechanism of this selective and successive suppression of the metallic component in the G-band and the intensities of the RBMs with increasing oxidation state requires a more thorough investigation.

In order to understand this phenomena more clearly, the G-band was deconvoluted into a single BWF line shape, one metallic and four semiconducting components in the Lorentzian shape.[17] The large BWF component (left shaded region) of the G-band, which represents a long energy tail at the lower energy side in the pristine sample, is evidence of the abundance in the metallic SWCNTs.[16] This successive modification of the metallic component with increasing oxidation state can be understood by the fact that electrons are extracted from the metallic CNTs to the adsorbates through oxidation. Nevertheless, the peak position of the $G^+$-band near 1592 $cm^{-1}$ at 633 nm, which represents the semiconducting nanotubes, was downshifted at an oxidation state of +1 and +3. In this case, the electrons were transferred from the adsorbates to the semiconducting CNTs. This is in contrast to the typical oxidation effect, which showed the uptake of electrons and the corresponding upshift in the $G^+$-band.[8] These observations reflect the general rule that a semiconductor has larger electron affinity than a metal.[18] This might be related to the fact that the high redox potential at low oxidation state can promote a strong interaction with the CNTs, which acts as a rate-limiting step for further oxidation.

On the other hand, no peak shift in the $G^+$-band was observed in the case of samples with exclusively semiconducting SWCNTs at 514 nm. Therefore, the metallic SWCNTs reacted selectively with the chlorine oxoanions, particularly at a low oxidation state, and were converted to semiconducting ones with pseudo band gap opening,[19] whereas the semiconducting SWCNTs were quite inert to these oxidants over the entire range of oxidation states. The degree of peak shift in the $G^+$-band is also strongly dependent on the concentration of oxidant (see Figure S1 and S2 in Supporting Information). The $G^+$ peak position was upshifted gradually with increasing concentration of perchlorate (oxidation state +7). An optimum concentration is needed to selectively modify the metallic SWCNTs with a minimum

(17) Brown, S. D. M.; Jorio, A.; Corio, P.; Dresselhaus, M. S.; Dresselhaus, G.; Saito, R.; Kneipp, K. *Phys. Rev. B* **2001**, *63*, 155414.

(18) Chattopadhyay, D.; Galeska, I.; Papadimitrakopoulos, F. *J. Am. Chem. Soc.* **2003**, *125*, 3307.

(19) Strano, M. S.; Dyke, C. A.; Usrey, M. L.; Barone, P. W.; Allen, M. J.; Shan, H.; Kittrell, C.; Hauge, R. H.; Tour, J. M.; Smalley, R. E. *Science* **2003**, *301*, 1519.

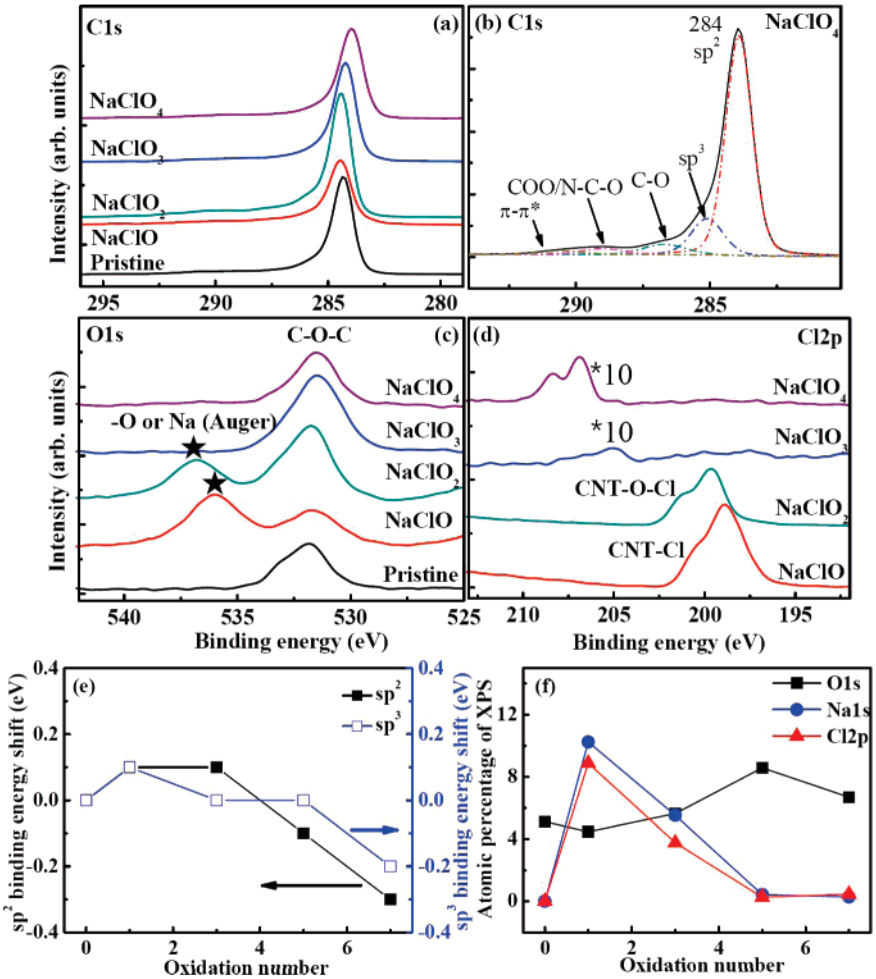


***Figure 3.*** XPS analysis of (a) C1s, (b) fitted C1s about $NaClO_4$, (c) O1s, and (d) Cl2p core peaks after the oxidizing agent treatment. (e) Binding energy shift in the sp2 and sp3 peaks of C1s with respect to the pristine sample. (f) Atomic percentage of O1s (■), Na1s (●), and Cl2p (▲) determined from XPS quantitative analyses.

change in the semiconducting SWCNTs. The metallicity of the SWCNTs was fully recovered by thermal annealing at 600 °C under Ar atmosphere with minimum damage the nanotubes (see Figure S3 in Supporting Information). This suggests that the reaction involves physisorption rather than chemisorption.

In order to determine how this selective modification of metallic SWCNTs affects the sheet resistance, the sheet resistance was measured as a function of the oxidation state (Figure 2b). The sheet resistance was increased by approximately 30% at an oxidation state of 1 and decreased further with increasing oxidation state. The areal intensity of the metallic and semiconducting components was also extracted by deconvoluting the G-band (Figure 2c). It should be noted that there was some correlation between the two curves with the exception of the first two points. In general, the sheet resistance of the random network SWCNTs is determined by the sum of resistances of the intrinsic SWCNT network and tube−tube contact. The tube−tube contact is composed of metal−metal and semiconductor−semiconductor junctions that give ohmic behavior and a metal−semiconductor junction that forms a Schottky barrier.[20] The conversion of metallic SWCNTs to semiconducting ones at high oxidation state might result in an increase in the resistance of the intrinsic SWCNTs but reduces the contact resistance significantly by decreasing the number of metal−semiconductor junctions. Nevertheless, this argument is not applicable at an oxidation state of 1; that is, the resistance increased compared with the pristine sample. This will be discussed later.

XPS analysis was performed to understand the effect of oxidation more clearly (Figure 3). A thorough analysis of the C1s core peak provides valuable information regarding the nature of carbon bonding. For the pristine CNT film, the C1s spectrum was mainly composed of a large $sp^2$ carbon component at 284.3 eV, a small $sp^3$ carbon peak at 285.1 eV, oxygen-related groups, and $\pi-\pi^*$ plasmon satellite.[21] The oxidation effect could be identified by the C1s peak shift shown in Figure 3a. In addition, an extra COO/N−C−O related peak was observed in the case of the oxidized samples, as shown in Figure 3b.[22] In the case of oxidation by NaClO and $NaClO_2$, a new peak appeared at approximately 534∼538 eV, which was assigned to chemisorbed oxygen and/or water. However, the precise assignment of the O1s peak at higher binding energies presents some difficulties due to the presence of a sodium Auger line in

(20) Fuhrer, M. S.; Nygard, J.; Shih, L.; Forero, M.; Yoon, Y. G.; Mazzoni, M. S. C.; Choi, H. J.; Ihm, J. S.; Louie, S. G.; Zettl, A.; McEuen, P. L. *Science* **2000**, *288*, 494.

(21) (a) McFeely, F. R.; Kowalczyk, S. P.; Ley, L.; Cavell, R. G.; Pollak, R. A.; Shiriley, D. A. *Phys. Rev. B* **1974**, *9*, 5268. (b) Diaz, J.; Paolicelli, G.; Ferrer, S.; Comin, F. *Phys. Rev. B* **1996**, *54*, 8064.

(22) Moulder, J. F.; Stickle, W. F.; Sobol, P. E.; Bomben, K. D. *Handbook of X-ray Photoelectron Spectroscopy*; Physical Electronics Inc.: 1992.

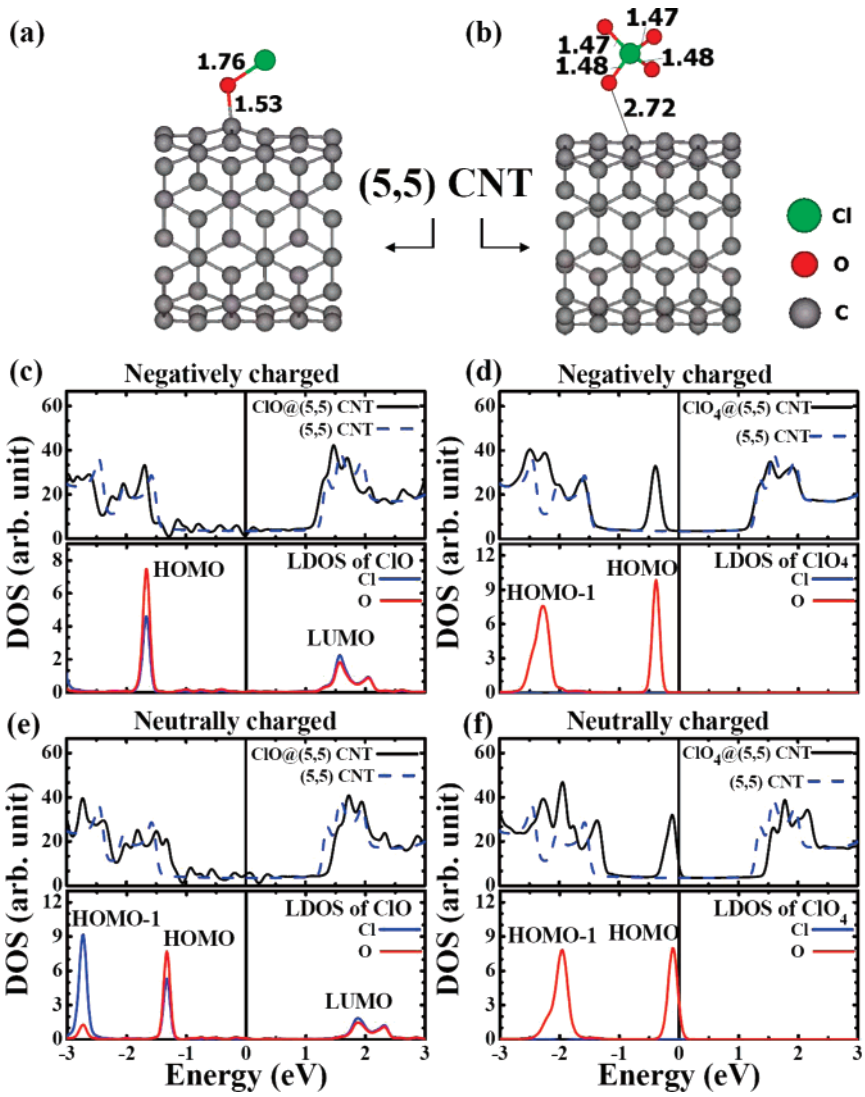


***Figure 4.*** (a, b) Fully relaxed geometries of both ClO and $ClO_4$ on a (5,5) nanotube; (c, d) the case of a negatively charged state; (e, f) the case of a neutrally charged state.

this energy range.[22] No such peaks were observed at the high oxidation states. Similar Cl2p peaks were present. The Cl2p peak observed near 199 eV was attributed to the presence of salt in the samples (NaCl). This was confirmed by the Na1s peak around ~1072 eV (not shown here). In case of $NaClO_2$, another peak near 1073 eV (Na−O) in Na1s and 200 eV in Cl2p were observed, which is due to the presence of Na−O−Cl.[22]

Figure 3e,f summarizes the characteristics of the XPS spectra. Both peaks related to $sp^2$ and $sp^3$ carbon were upshifted by approximately 0.1 eV at the low oxidation states of +1 and +3, whereas they were downshifted at the high oxidation states, which is the case with a typical downshift in p-doped CNTs.[7,10] The atomic percentage of oxygen did not change much independent of the oxidation states, whereas the atomic percentage of sodium and chlorine increased significantly at low oxidation state of +1. This may be the origin of the upshift of C1s: the charges are transferred to CNTs from adsorbates. Thus the p-type carrier is compensated by an effective n-doping, resulting in the reduction of sheet resistance as observed in Figure 2b. On the other hand, there was no appreciable sodium and chlorine remaining at the high oxidation states of +5 and +7. This suggests that the reaction process involves a complicated pathway of adsorption and decomposition into the final products such as sodium chloride and oxygen species.

Theoretical density functional calculations were used to further understand the adsorption process. Since the different reaction processes between the low and high oxidation states appear to be involved, ClO and $ClO_4$ were chosen for the calculations in order to understand the underlying mechanism. Figure 4a,b shows the fully relaxed geometries of both species on (5,5) nanotubes in the neutral state.[23] The local geometries were relatively unaffected even for the negatively charged states. Two intriguing phenomena were observed. First, ClO adsorbs strongly to the CNT wall via the oxygen atom with a binding energy of 0.8 eV. This structure is stable and the adjacent sodium ions will be attached via the oxygen atoms. On the other hand, $ClO_4$ adsorbs relatively weakly via oxygen atom with the CNT wall with a binding energy of 0.2 eV. This originates from the steric hindrance by the adsorbed oxygen atom near the CNT

(23) The convergence was tested with a large diameter (10,10) nanotube. The changes in Cl−O and C−O bond lengths were negligible. The charge transfer difference was within 0.02 e but the direction of the charge transfer was the same as (5,5).

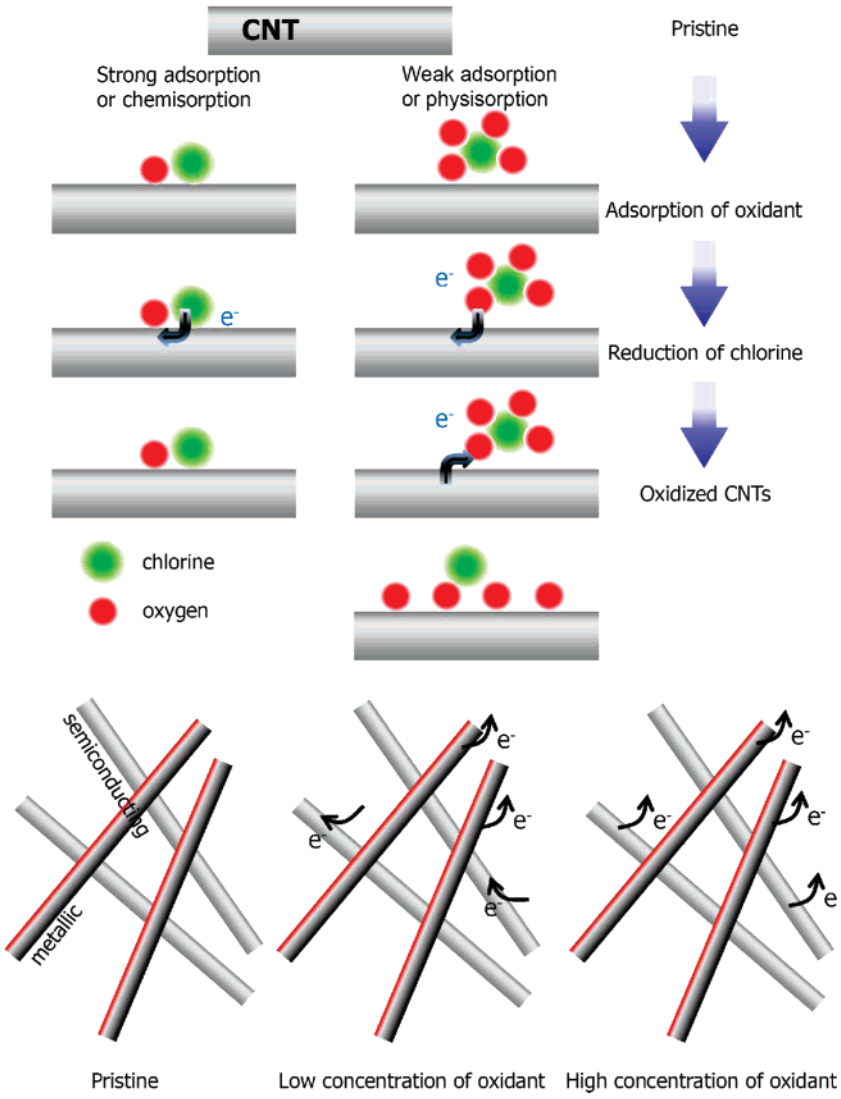


***Figure 5.*** Schematic diagram of the reaction pathway.

wall. Besides, the electric dipole moment of $ClO^-$ is about 10 times larger than that of $ClO_4^-$. This accounts for the difference of the adsorption characters of the two adsorbates. The weakly adsorbed $ClO_4$ could be further dissociated into $ClO_3$ due to the low redox potential, as shown in Table 1. Second, the Fermi level was downshifted (0.21 eV) in the case of ClO. The Fermi level was upshifted (0.71 eV) in the case of negatively charged state ($ClO^-$); that is, electrons were transferred from $ClO^-$ to the CNT. In contrast, the Fermi level was downshifted (0.68 eV) in the case of $ClO_4$, indicating the charge transfer from CNT to mostly oxygen atoms. The Fermi level was upshifted (0.19 eV) in the case of the negatively charged state ($ClO_4^-$). We also calculated the case of $ClO_4^{\delta-}$ ($\delta = 0.5$). Interestingly electrons were transferred from the CNT to mostly oxygen atoms similar to the neutral $ClO_4$. Because both peaks related to $sp^2$ and $sp^3$ carbon were upshifted at ClO but downshifted at $ClO_4$ in the XPS data, $ClO_4$ may exist in a smaller negatively charged state ($0 < \delta < 1$) than ClO in the same medium. However, the weakly bound $ClO_4$ may not necessarily be the final product after the reaction due to the low redox potential, as shown in Table 1.

Figure 5 shows a schematic diagram of the reaction pathways of chloro oxoanions on CNTs. The reaction involves mainly two steps: adsorption and reduction/oxidation. In the case of strong adsorption at the low oxidation states, the strongly adsorbed adsorbate will be reduced further. This might involve forming a sodium−oxygen−chloride complex. This complex will still remain on the CNT surface, as evidenced by XPS. In the case of weak adsorption of high oxidation states, $ClO_4$ may reduce to ClO through charge transfer with the CNTs due to the low redox potential, as expected from Table 1. As a consequence, the byproduct oxygen atoms might be adsorbed onto the surface in a form of a molecule by physisorption involving charge transfer from the CNTs to the oxygen molecules, as confirmed by the downshift in the sp-related peaks in XPS. The chlorine atoms may form a complex with the adjacent sodium atoms, which are likely to be desorbed due to the weak interaction with the CNTs, which was confirmed by XPS analysis. This charge transfer is also dependent on the concentration of the oxidants. At low concentration, the metallic SWCNTs release charges to the adsorbates, whereas the semiconducting SWCNTs extract charges from the adsorbates, as evidenced from the Raman spectra. On the other hand, at high concentrations, both metallic and semiconducting SWCNTs release charges to the adsorbates, which follow the general rule of oxidation by oxidants. The effect of such charge transfer to

the sheet conductance can be understood by a doping behavior. The pristine SWCNTs are usually p-doped due to the presence of ambient adsorbates. For the metallic SWCNTs, the depletion of electrons involves a pseudogap opening, which leads to a transformation from metallic to semiconducting SWCNTs.[19] This might increase the resistance of CNTs but decrease the number of metallic−semiconducting Schottky junctions, which eventually decreases the sheet conductance.[24−26] The extraction of electrons from semiconducting SWCNTs simply enhances the p-doping concentration, which further decreases the sheet resistance.

## 4. Conclusions

This study examined the effect of oxidation on CNTs by introducing chloro oxoanions with the chlorine atom at various oxidation states. At a low concentration of oxidants with a high oxidation state, selective oxidation was observed on the metallic carbon nanotubes with a minimal effect on the semiconducting nanotubes, where the charges are extracted mainly from the metallic nanotubes to the adsorbates. At a low concentration of oxidants, the oxidation behavior at a low oxidation state was quite different from that observed at a high oxidation state. The oxidation at a low oxidation state involves rather strong chemisorption and charge transfer from the adsorbates to CNTs. On the other hand, oxidation at a high oxidation state involves an intermediate physisorption that evolves to dissociate into further byproducts of the oxygen adsorbates, leaving charge transfer from the CNTs to adsorbates. The sheet resistance was reduced significantly when the p-doping behavior was dominant. The finding of selective doping on metallic SWCNTs with oxidation can be applied to the precise doping control of several electronic devices.

**Acknowledgment.** We acknowledge the financial support by the Korea Research Foundation Grant funded by the Korean Government through Star-faculty project, the KOSEF through CNNC at SKKU, Tera-level Nano Devices and in part by the MOE, MOCIE and MOLAB through the fostering project of the Lab of Excellence.

**Supporting Information Available:** Experimental procedures and Figures S1−S3. This material is available free of charge via the Internet at http://pubs.acs.org.

JA077449D

(24) Ouyang, M.; Huang, J.; Cheung, C. L.; Lieber, C. M. *Science* **2001**, *292*, 702.
(25) Sze, S. M. *Physics of Semiconductor Devices*, 2nd ed.; Wiley: New York, 1981; Chapt. 2.
(26) Kim, K. S.; Bae, D. J.; Kim, J. R.; Park, K. A.; Lim, S. C.; Kim, J.; Choi, W. B.; Park, C. Y.; Lee, Y. H. *Adv. Mater*. **2002**, *14*, 1818.